Pluto and Charon as Templates for Other Large Transneptunian Objects

W. M. Grundy

Lowell Observatory

Chapter 13 in *The Trans-Neptunian Solar System* pp. 291-305

Edited by D. Prialnik, M. A. Barucci, and L. A. Young

Elsevier (2020)

ISBN: 978-0-12-816490-7

DOI: 10.1016/B978-0-12-816490-7.00013-8

Abstract

Exotic landforms are created on Pluto through the action of highly volatile surface materials that can be mobilized by the small amounts of energy available from sunlight and from the decay of radioactive isotopes in Pluto's core. Although Charon is to small to have retained the volatiles that enable Pluto's continuing activity, it too was geologically active in the past. The processes that enable activity at the extremely cold temperatures prevalent on small bodies far from the Sun offer lessons for what sorts of processes might once have shaped, or even still be modifying the surfaces of other large, as-yet unexplored transneptunian bodies.

Introduction

Following its discovery in 1930, Pluto was seen by planetary scientists as a lone oddball, distinct from both the rocky planets and from the giant planets. Imagination of what its geology

might be like was initially limited by lack of experience with spacecraft exploration of comparable bodies. The 1989 Voyager II flyby of the Neptune system changed that, providing a key point of reference. Voyager's instruments revealed Neptune's largest satellite Triton to be a spectacularly complex world with a wealth of geological features, some of them bearing little resemblance to landforms seen elsewhere in the solar system and some pointing to recent or even ongoing geologic activity (e.g., Smith et al. 1989; Croft et al. 1995; Schenk and Zahnle 2007). For a generation of planetary scientists, Triton served as a template for the surprises Pluto might hold.

Triton and Pluto are similar in many ways. They are comparable in size, with diameters of 2707 and 2377 km for Triton and Pluto, respectively. Their bulk densities are similar too, being intermediate between the bulk densities of water ice and of rock, more rock-rich than the mid-sized icy satellites of Saturn and Uranus. Like Pluto, and unlike other large icy satellites of the giant planets, Triton is thought to have originated in the outer protoplanetary nebula prior to its capture into orbit around Neptune (e.g., McKinnon 1984; Lunine 1993; Agnor and Hamilton, 2006; Nogueira et al. 2011). Triton and Pluto both have thin, nitrogen-dominated atmospheres (e.g., Hubbard et al. 1988; Tyler et al. 1989), along with the same volatile ices on their surfaces: nitrogen N_2, methane CH_4, and carbon monoxide CO (e.g., Cruikshank et al. 1993; Owen et al. 1993; Cruikshank et al. 2005), mobile on seasonal timescales (e.g., Trafton et al. 1998). Of course, there were differences, too, making Triton an imperfect template. For instance, Triton's orbit around Neptune offers a source of internal heating via tidal dissipation, unavailable to Pluto. And Triton's location within Neptune's magnetosphere puts it in a different charged particle environment from Pluto's setting in the solar wind. Nonetheless, Triton's exotic and enigmatic geology pointed to the diversity of features that might be expected at Pluto, and helped spur interest in sending a spacecraft to explore it (Neufeld 2014).

NASA's New Horizons spacecraft flew through the Pluto system in July 2015, sending back a wealth of data from its seven scientific instruments (Stern et al. 2015). This chapter will show data from two of the instruments. The LOng-Range Reconnaissance Imager (LORRI) is a panchromatic 1k × 1k CCD detector mounted on an 8" telescope (Cheng et al. 2008). The Ralph instrument consists of two components, the Multi-spectral Visible Imaging Camera (MVIC), and the Linear Etalon Imaging Spectral Array (LEISA; Reuter et al. 2008). MVIC provides wide field of view CCD imaging in 4 color filter channels plus panchromatic channels. LEISA

performs spectral imaging at wavelengths from 1.25 to 2.5 μm at a spectral resolution ($\lambda/\Delta\lambda$) of about 240.

This chapter will examine the Pluto system's distinctive suite of features revealed by New Horizons and consider how its distinct types of activity might provide templates for revelations from future exploration of other large transneptunian bodies.

Powering planetary activity

Planetary activity requires the presence of materials that can be mobilized along with the energy to mobilize them. The primary source of energy in the Pluto system is sunlight, despite Pluto's orbiting at a mean distance 39 times further from the Sun than Earth does. Pluto's version of the solar "constant" ranges from 1.52 W m^{-2} at perihelion to 0.57 W m^{-2} at aphelion. Additional energy is available from the decay of radioactive isotopes in Pluto's interior, chiefly ^{232}Th and ^{238}U, with smaller contributions from ^{235}U and ^{40}K which would have been more important early in Pluto's history. If these radionuclides are present in chondritic abundances in rock that accounts for 65.5% of Pluto's total mass (and 59% of Charon's), their decay would contribute about 0.003 W m^{-2} at Pluto's surface and about half that at Charon's surface (McKinnon et al. 2017). These energy sources are minuscule compared to their counterparts on Earth (1361 W m^{-2} for the terrestrial solar constant and about 0.09 W m^{-2} geothermal heat from a combination of radioisotope decay and residual heat from Earth's formation and differentiation; Davies and Davies 2010). Yet they are sufficient to make Pluto geologically active thanks to the presence on Pluto of abundant volatile materials N_2, CH_4, and CO. These form weakly-bonded solid ices that are readily mobilized with modest energy inputs. The next sections review some of Pluto's more striking geological features enabled by the mobilization of these volatile materials, and then consider a few of Charon's features.

Pluto

The diversity of processes shaping Pluto's surface is hinted at by the topography and color views in Fig. 1. Many distinct landforms are produced.

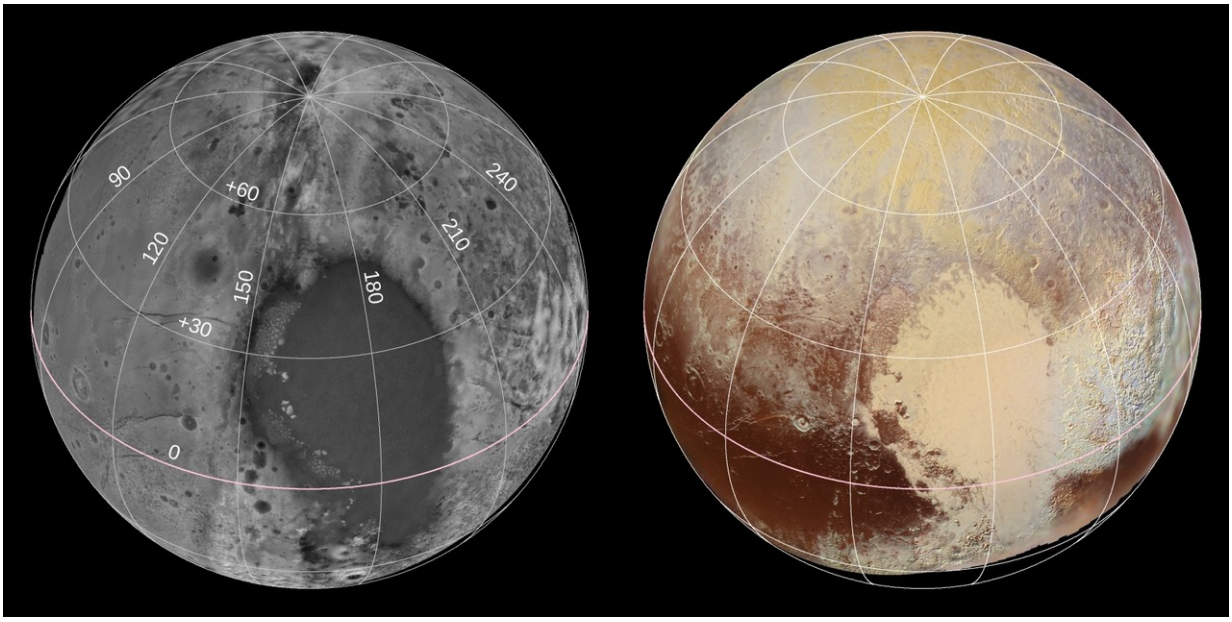

Figure 1. Topography (left) and color mosaic (right) of Pluto in orthographic projection centered on the encounter hemisphere. The topographic data (Schenk et al. 2018a) are scaled from 4 km below Pluto's 1188.3 km mean radius (black) to 10 km above the mean radius (white). The color image is made from three of the four MVIC filters: 400-550 nm displayed in blue, 540-700 nm displayed in green, and 780-975 nm displayed in red.

The bladed terrain of Tartarus Dorsa[1] (Fig. 2) stands out as a prominent high-altitude region in the topographic map near the eastern edge of the encounter hemisphere. Broad swells are separated by deep troughs. Perched atop the swells are narrower blades, oriented roughly north-south and spaced from 3 to 7 km apart. The blades are up to 1 km in height, with the largest of them occurring near the crests of the broader swells (Moore et al. 2016, 2018). Few if any craters cut into the bladed terrain, suggesting a recent or ongoing formation process (Moore et al. 2018). The composition of the blades appears to be dominated by CH_4 ice, the least volatile of Pluto's three volatile ices (Grundy et al. 2016a; Schmitt et al. 2017; Earle et al. 2018). Bladed terrain shows a distinctive coloration in MVIC images, and that color extends much further to the east along the equator in lower resolution approach images (Olkin et al. 2017), suggesting that bladed terrain is much more widespread on the non-encounter hemisphere of Pluto. The blades are hypothesized to be analogous to terrestrial penitentes (Moores et al. 2017; Moore et al. 2018). Penitentes are jagged residual features formed as a thick deposit of snow or ice sublimates away, with sunlight controlling where sublimation occurs, possibly in concert with

1 Pluto system feature names used here include a mix of informal and officially approved names.

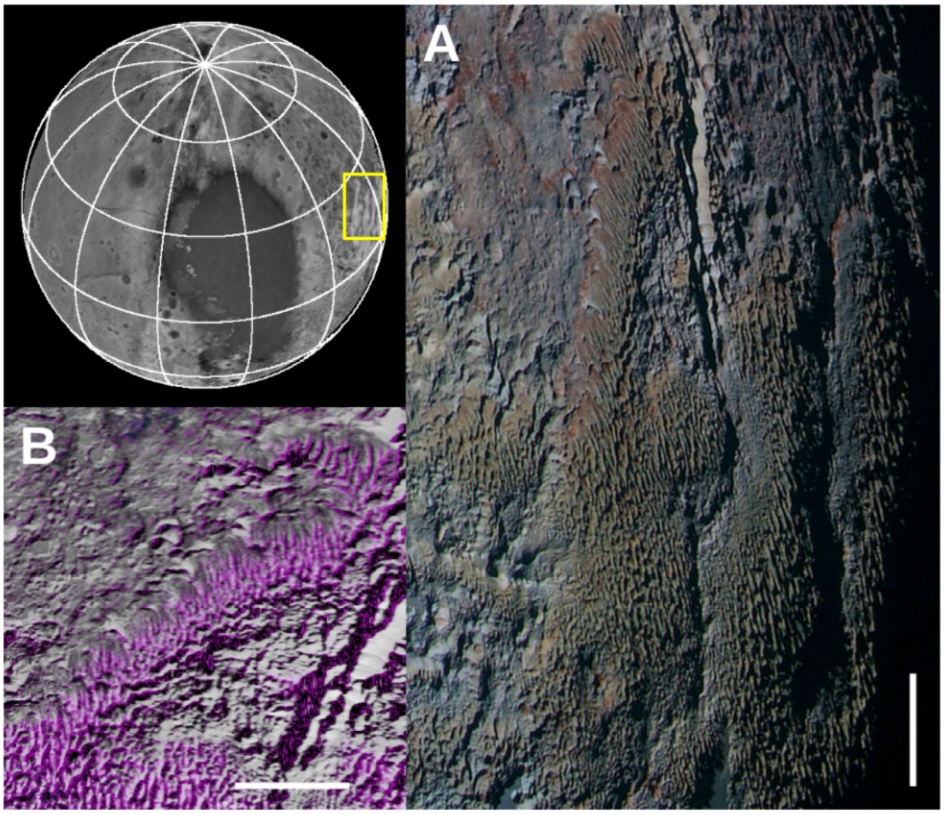

Figure 2. Bladed terrain location indicated by yellow box on the elevation map from Fig. 1. (A) Oblique MVIC color image and (B) CH_4 ice absorption map (Earle et al. 2018) highlighted in magenta on the panchromatic base map (Schenk et al. 2018a). Scale bars are 50 km.

wind. How the thick layer of CH_4 ice from which the blades were carved came to be deposited in the first place remains unclear, but could be related to the several million year "mega-season" cycles of Pluto's obliquity and longitude of perihelion (e.g., Dobrovolskis and Harris 1983; Earle and Binzel 2015; Bertrand et al. 2018).

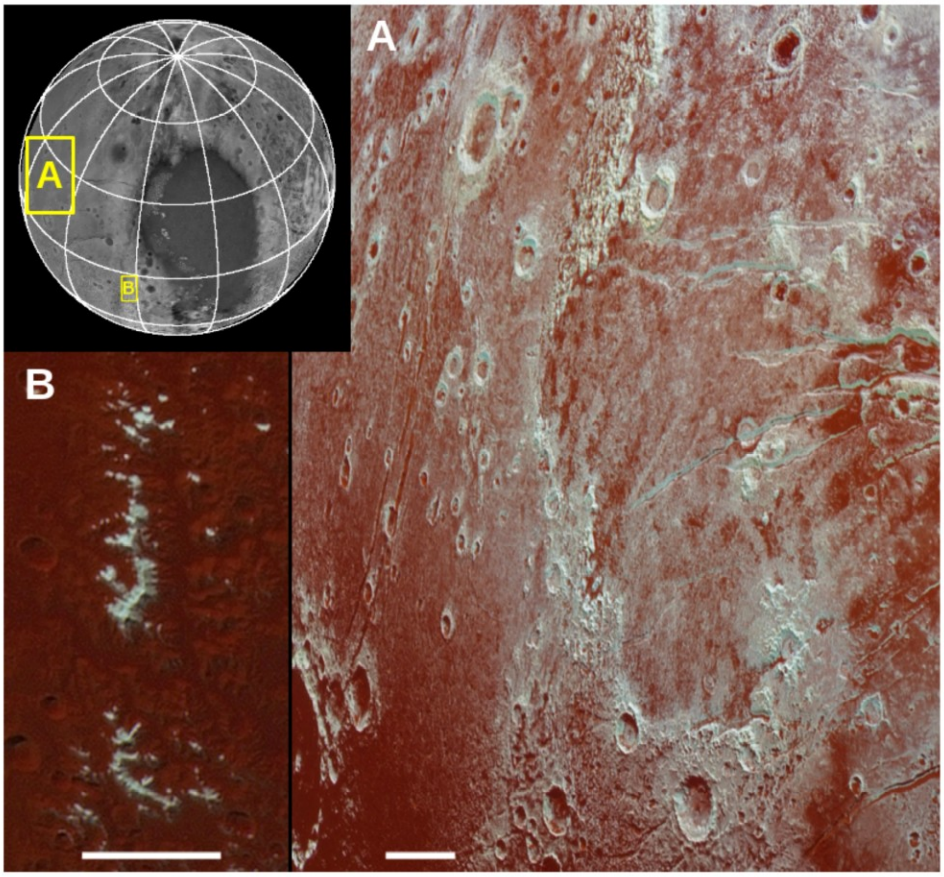

Figure 3. MVIC color images of bright CH_4 ice on the uplands of Piri Rupes and numerous crater rims in Vega Terra (A) and on peaks of Enrique Montes (B). Scale bars are about 50 km.

Elsewhere at low latitudes, CH_4 ice can be seen occupying high altitude sites such as the crests of mountains and the rims of craters (Fig. 3). It is unclear if these outcrops are the last remnants of a once-widespread deposit, or the result of preferential deposition of CH_4 frost on high and thus cold regions (e.g., Grundy et al. 2016a; Moore et al. 2017). If the latter, that could suggest an alternate formation scenario for the bladed terrain, that the blades are built up through deposition of CH_4 at high altitudes rather than eroded through sunlight-driven sublimation. Or perhaps both processes work in tandem or alternating with Pluto's climate cycles.

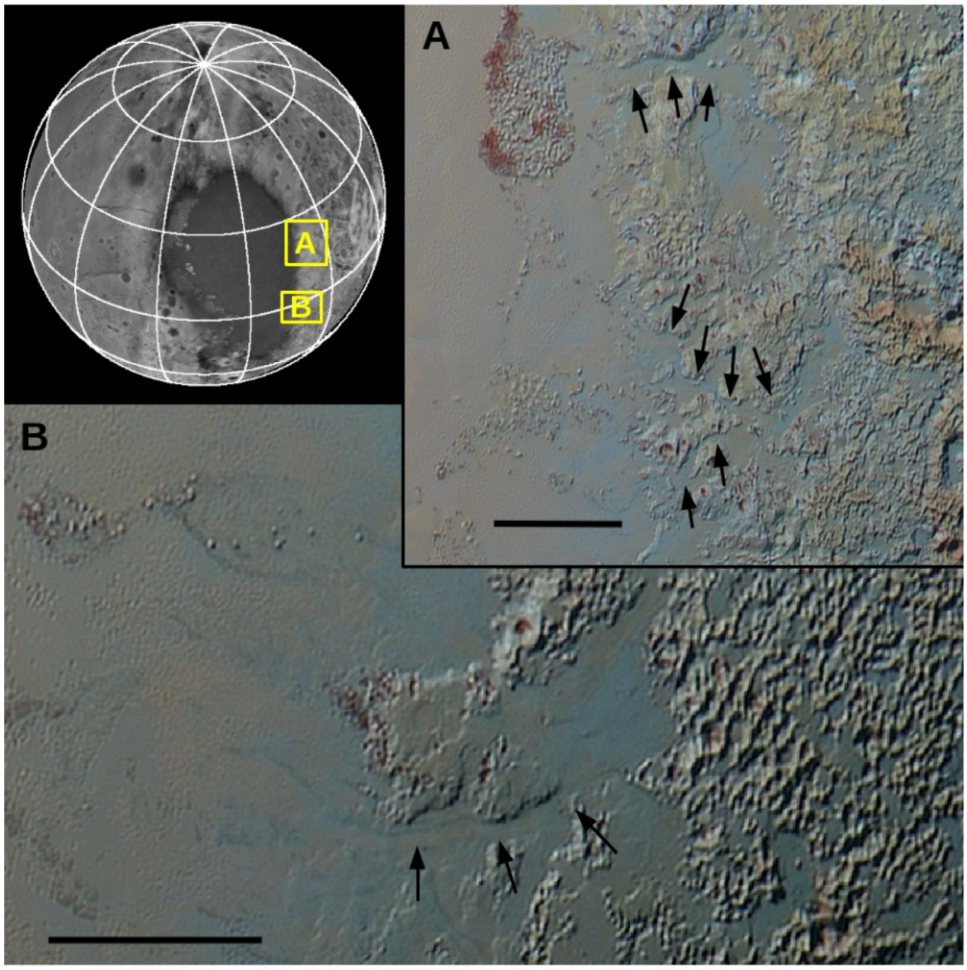

Figure 4. MVIC color images of valley glaciers flowing into Sputnik Planitia from the east. Scale bars are 50 km.

At Pluto surface temperatures N_2 ice is much less rigid than CH_4 ice. Under the influence of Pluto's weak gravity (6.3% of Earth's) it flows downhill like water ice does in valley glaciers on Earth (Umurhan et al. 2017). Several currently active valley glaciers can be seen in Tombaugh Regio, the large, bright feature on Pluto's encounter hemisphere (Fig. 4). These flow westward, transporting N_2 ice from higher elevations in eastern Tombaugh Regio down into the large basin of Sputnik Planitia, carving valleys. The source of the N_2 ice feeding these glaciers appears to be seasonal cycles of sublimation, atmospheric transport, and condensation (e.g., Bertrand et al. 2018). N_2 glaciers on Pluto have several key differences from H_2O glaciers on Earth. First, if N_2 were to melt within the glacier, the liquid is less dense than N_2 ice, so it will percolate upward toward the cold surface of the glacier, where it would re-freeze or perhaps erupt as jets or geysers. H_2O liquid is more dense than ice, so any liquid that forms in a

terrestrial glacier drains downward toward the base of the glacier, where it can help lubricate the glacier's progress, and also help erode the bedrock through freeze-thaw cycles. Terrestrial rocks are much denser than H_2O ice, so glaciers on Earth generally flow over the rocky substrate. But on Pluto, the bedrock is mostly H_2O ice, which is slightly less dense than N_2 ice. This density inversion suggests that boulders of H_2O ice bedrock could rise up through the glacier, and that glaciers might exploit fractures to flow down into the ground.

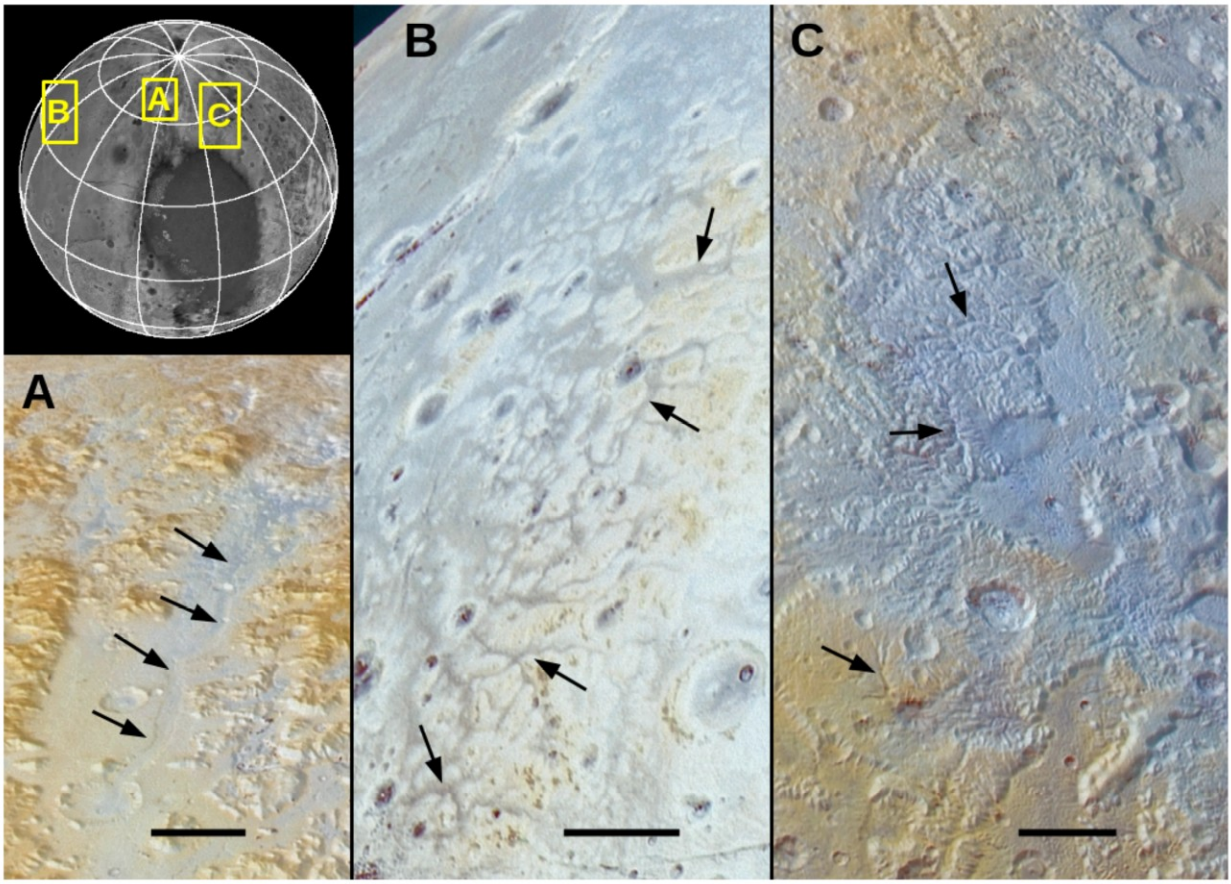

Figure 5. MVIC color images of channels with a variety of morphologies. Scale bars are 50 km.

Additional channels can be seen in various locations across Pluto (Fig. 5), exhibiting a range of morphologies (Moore et al. 2016; Howard et al. 2017a). It is unclear whether these result from past epochs of glacial erosion, or from sub-glacial or subsurface liquid flow, or even from surface liquid erosion during climatic extremes of temperature and pressure (e.g., Stern et al. 2017).

Pluto's largest glacier by far occupies Sputnik Planitia, the ~1000 km wide ancient impact basin that forms the western half of Tombaugh Regio. Sputnik is partly filled with N_2 ice, along

with small amounts of CO and CH_4 (Stern et al. 2015; Moore et al. 2016; Protopapa et al. 2017). This deposit is thick, probably more than a kilometer deep, and N_2 ice is a good thermal insulator, so the meager heat from Pluto's interior is sufficient to drive solid state convective overturn (McKinnon et al. 2016; Trowbridge et al. 2016). This churning continually refreshes the surface, keeping it free of impact craters. The nearly level surface is marked by a distinctive pattern of polygonal convection cells some 10s of km across (White et al. 2017). Warm ice rises in the centers of the cells and cold ice sinks along the margins (Fig. 6). This type of solid state convective overturn is not seen in terrestrial glaciers, despite the much greater energy available from geothermal heat, and is unlike anything seen elsewhere in the solar system so far.

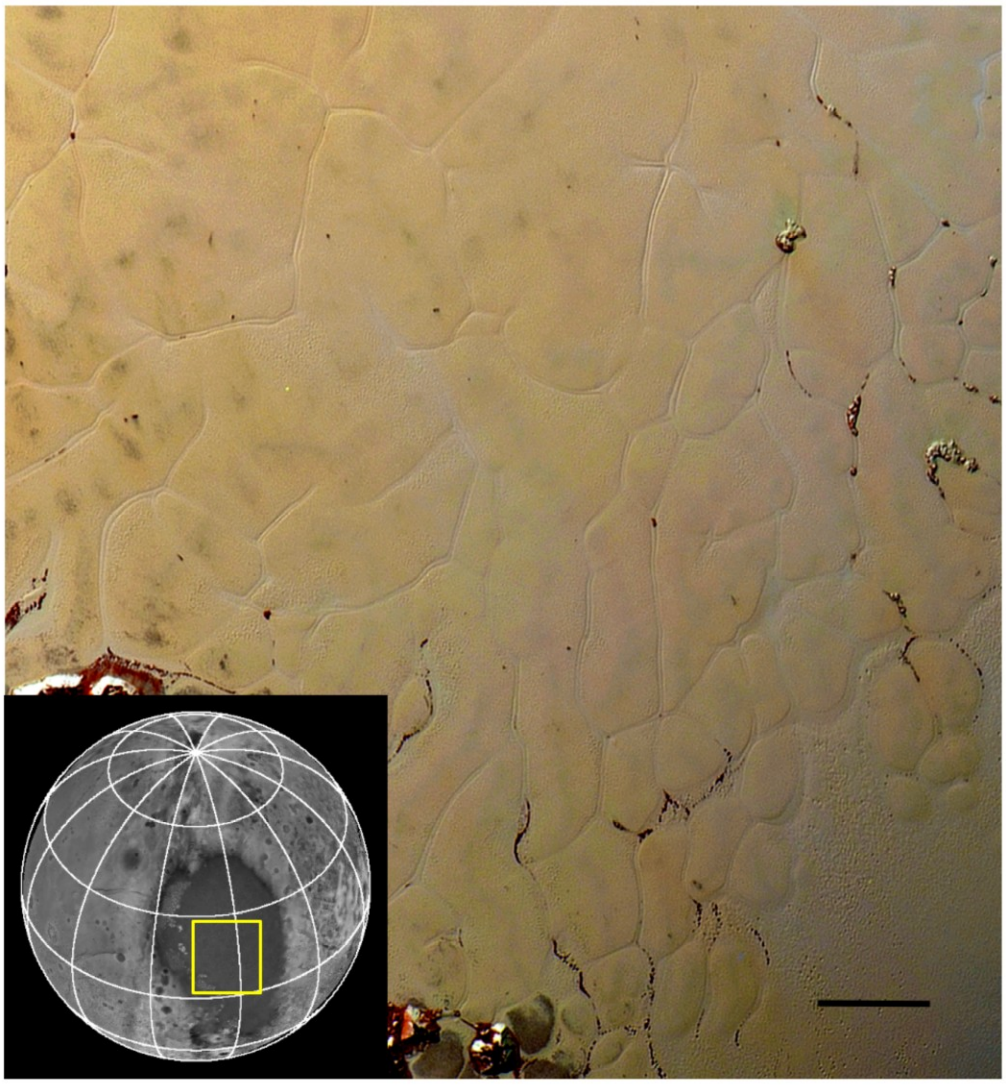

Figure 6. Contrast enhanced MVIC color image of convection cells in Sputnik Planitia. Scale bar is 50 km.

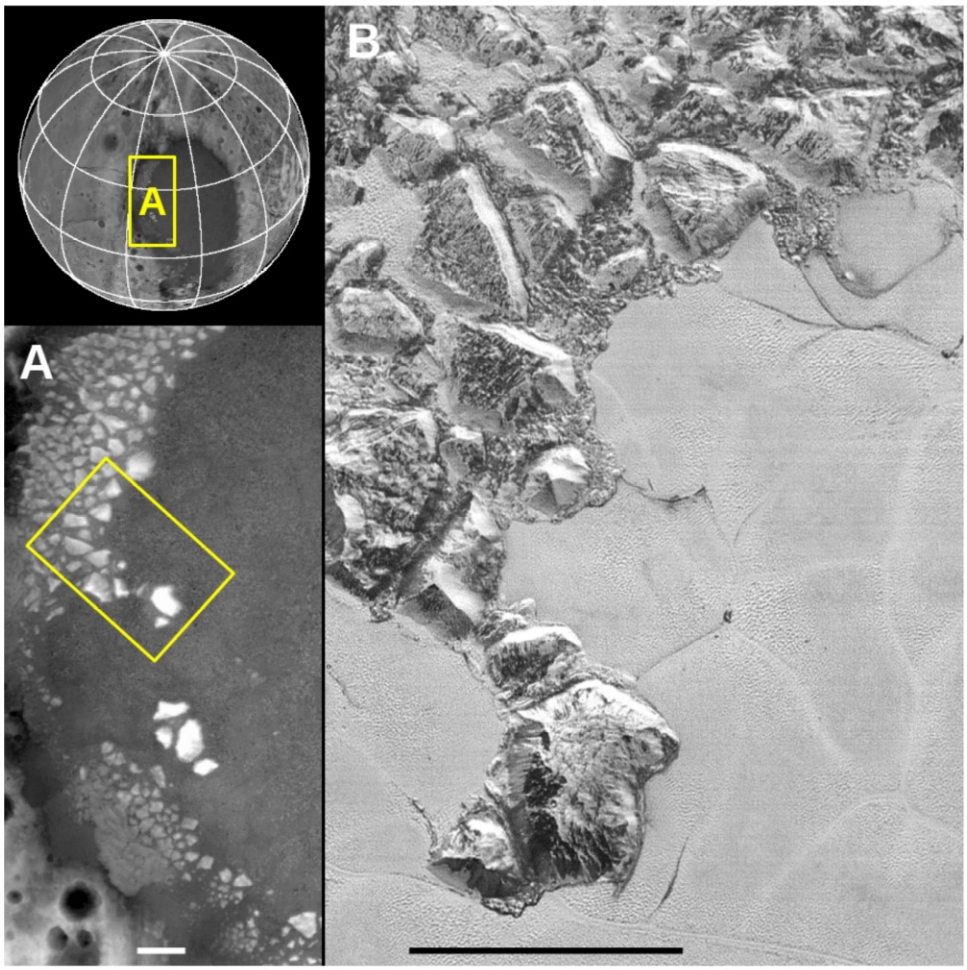

Figure 7. Mountain blocks rising out of Sputnik Planitia. (A) Topographic map scaled from −2.5 km (black) to +2.5 km (white) relative to Pluto's mean radius of 1188.3 km (Nimmo et al. 2017; Schenk et al. 2018a). (B) High resolution LORRI panchromatic image showing details of the region in the yellow box from (A). Scale bars are 50 km.

Rugged mountains jut up from the western side of Sputnik Planitia (Fig. 7), including Al-Idrisi, Zheng He, Baré, Hillary, and Tenzing Montes. These are thought to be blocks of Pluto's crust that were buoyantly supported by the N_2 ice glacier, enabling them to shift and rotate (Stern et al. 2015; Moore et al. 2016). The density contrast between H_2O and N_2 ices is small, so if these mountains are made of water ice, only the tips of the bergs should protrude above the N_2 surface. That seems inconsistent with their close proximity to one another. Possible explanations include the level of the N_2 ice having receded, exposing more of the roots of the mountains, or their being partly composed of much lower density CH_4 ice that would float higher in the N_2 glacier.

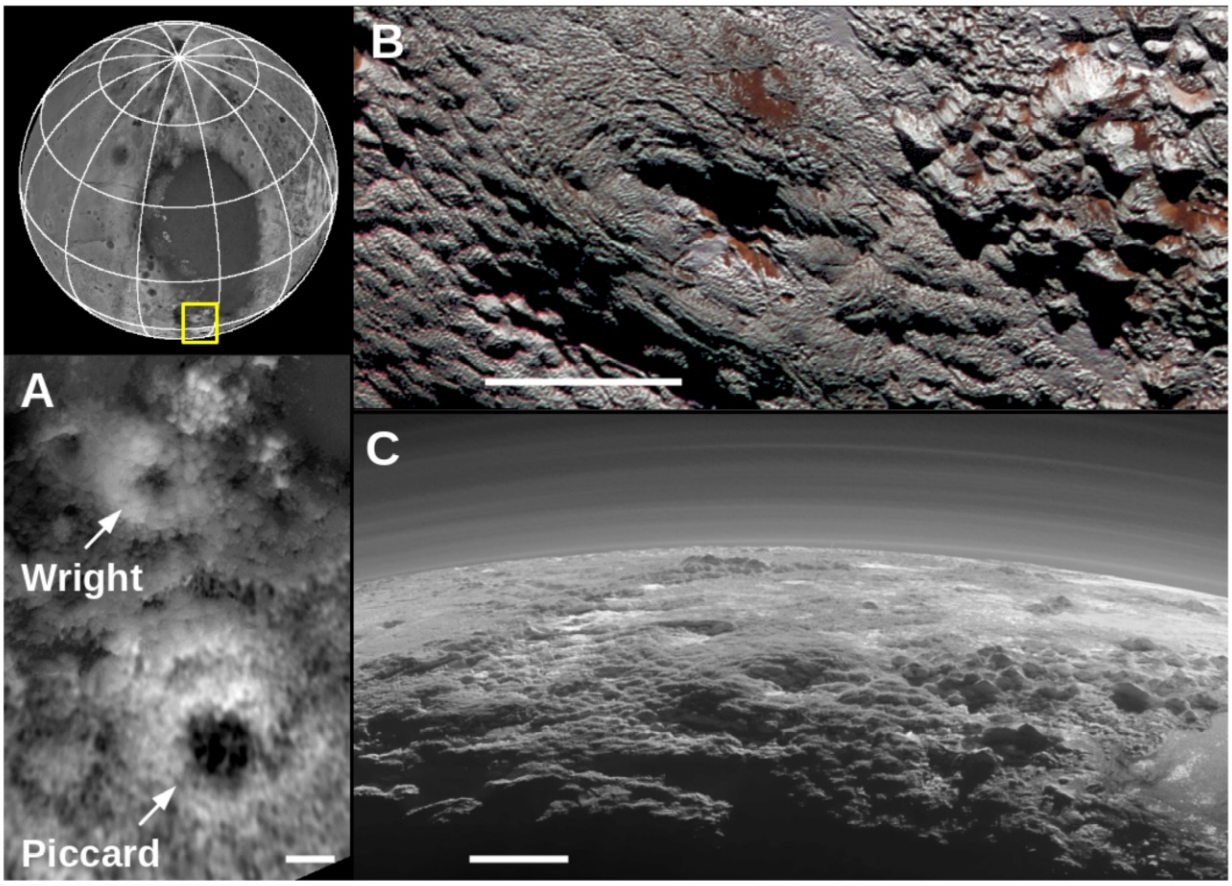

Figure 8. Cryovolcanoes Wright and Piccard Mons. (A) Topographic map scaled from −3 km (black) to +5 km (white) relative to Pluto's mean radius of 1188.3 km (Nimmo et al. 2017; Schenk et al. 2018a). (B) MVIC color view of Wright Mons. (C) High phase oblique MVIC panchromatic view of Wright Mons and nearby mountains, showing atmospheric haze layers above the limb. Scale bars are approximately 50 km.

Wright Mons and Piccard Mons are a pair of large, circular structures towering over the landscape in the south of the encounter hemisphere (Fig. 8). With their deep central pits and peculiarly hummocky texture, these features have been identified as cryovolcanoes (Moore et al. 2016). The paucity of impact craters marring their flanks suggests they were active relatively recently in geological time. The details of how the volcanoes are powered and what materials erupt from them remain unknown. Since liquid H_2O is more dense than H_2O ice, something else would have to be influencing it to make it erupt at the surface. One possibility is dissolved gases that come out of solution as the liquid rises, creating expanding bubbles (e.g., Neveu et al. 2015). Another is compression of a residual liquid pocket as an interior H_2O ocean expands on freezing. Other more exotic scenarios have been discussed, including subsurface circulation of more

volatile fluids involving N_2, CO, or CH_4 that could perhaps blast local H_2O bedrock out as they explosively escape from below the surface. Other small pits, and clusters of pits on Pluto might be the result of eruptive processes, too (Howard et al. 2017b; see Fig. 9). Some of these are surrounded by relatively clean H_2O ice (Schmitt et al. 2017; Cook et al. 2019). Since H_2O ice is inert in Pluto's surface environment, exposed H_2O ice should soon become coated by the volatile ices, along with the dark organic haze that is continually settling out of Pluto's atmosphere (Cheng et al. 2017; Grundy et al. 2018), implying relatively recent or even ongoing activity.

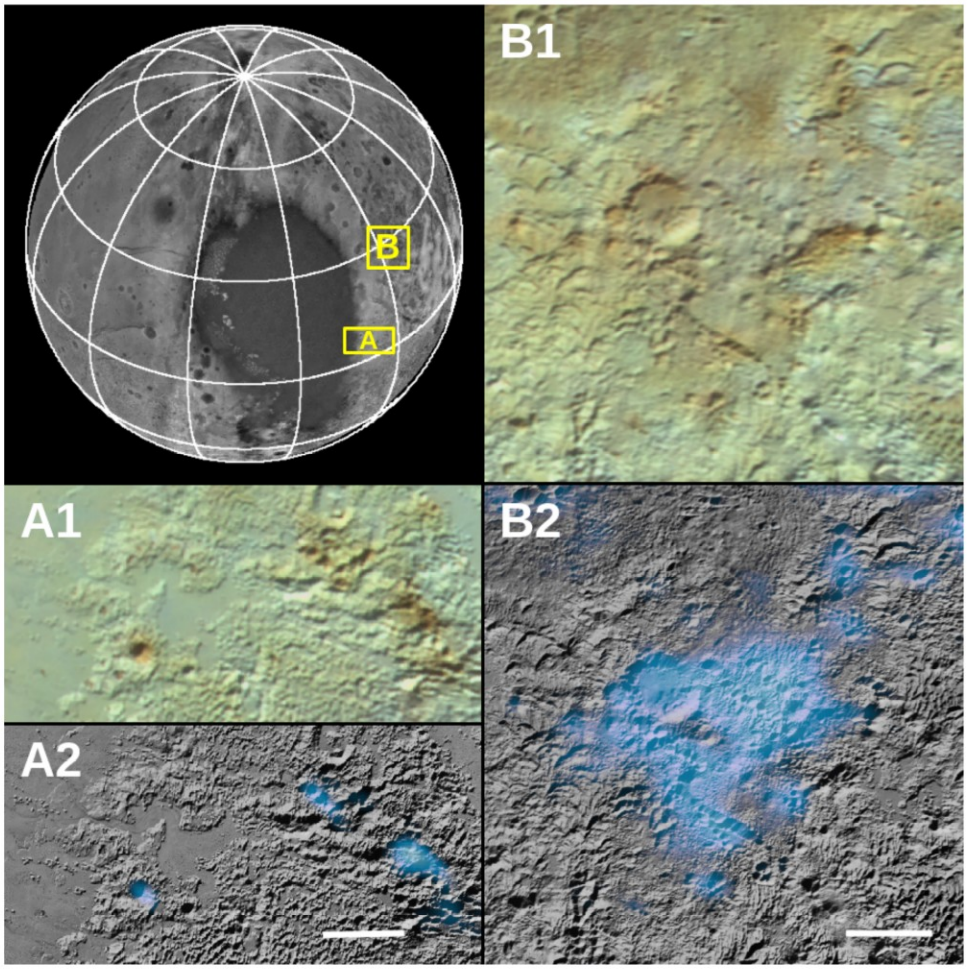

Figure 9. Pits, sometimes occurring in clusters or chains in eastern Tombaugh Regio. A1 and B1 panels show MVIC color. Some pits are associated with H_2O ice deposits (Schmitt et al. 2017; Cook et al. 2019), as indicated by the blue overlay on the base map in A2 and B2. The H_2O ice is often, but not always associated with reddish coloration in the MVIC color images. The large crater in (B) is Pulfrich, and the associated H_2O-rich region is Supay Facula. Scale bars are 50 km.

Charon

Charon's surface lacks the abundant volatile ices that enable much of Pluto's geological activity. It's surface gravity, just 2.9% of Earth's, is insufficient to prevent molecules like N_2 and CH_4 from escaping to space (e.g., Schaller and Brown 2007a). Abundant impact craters attest to an ancient age for Charon's surface. Yet there is also clear evidence for past activity that could provide useful hints to the sorts of geology we might find on comparably-sized transneptunian objects. Charon's activity involved H_2O, a material that is far less volatile than those enabling on-going activity on Pluto, but is thought to have benefited from the presence of various anti-freezes such as ammonia, alcohol, and salts, as well as higher abundances of radioactive elements leading to greater internal heat in the past (e.g., Desch and Neveu 2017).

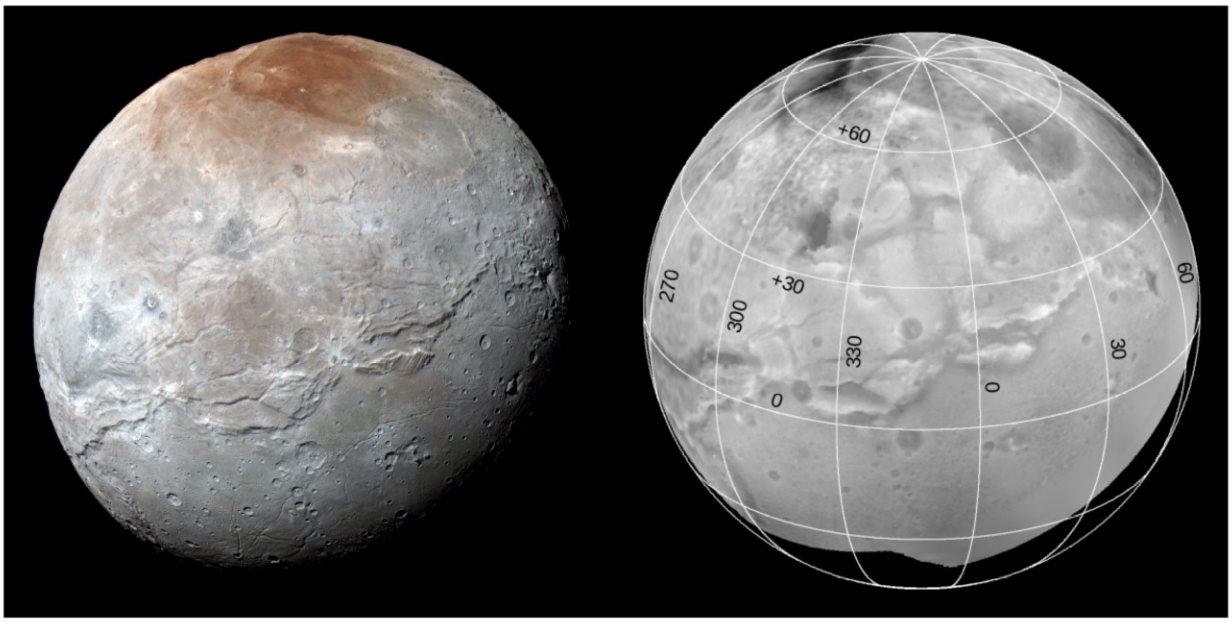

Figure 10. Charon MVIC color (left) and topographic map (right) of the encounter hemisphere, scaled from −10 km (black) to +5 km (white) relative to Charon's mean radius of 606.0 km (Nimmo et al. 2017; Schenk et al. 2018b).

A striking feature of Charon's encounter hemisphere (Fig. 10) is the dichotomy between the battered-looking northern hemisphere (Oz Terra), and the smoother southern hemisphere (Vulcan Planitia), separated by a belt of rugged cliffs and canyons of tectonic origin (e.g., Moore et al. 2016; Beyer et al. 2017; Schenk et al. 2018b). Vulcan Planitia's surface appears to have been flooded by a vast cryolava eruption. Several features suggest it was an extremely viscous flow, including mountains surrounded by moats, as well as a moat along the northern perimeter

of the planitia, suggesting a thick slurry or even glacier-like solid-state flow, rather than a liquid. One scenario involves break-up and foundering of crustal blocks into a warm, softer mantle which oozed up around the blocks, submerging some of them completely, but leaving others protruding through in places.

Oz Terra has dramatic tectonic features, too. They are hard to discern in the images, but stand out in the topographic map (Fig. 10) as a network of deep chasms separating high-standing blocks. This region of crust evidently did not completely founder as in Vulcan Planitia. Its more degraded appearance suggests the blocks in Oz Terra formed during an earlier episode. Freezing of an internal ocean is a probable explanation, since as the water freezes, it expands. The resulting extensional tectonics created horsts separated by grabens, similar to those seen on the uranian satellite Ariel (e.g., Beyer et al. 2017; Schenk et al. 2018b). Models show that after Charon's internal ocean freezes, radiogenic heat from the core is less able to escape to the surface, leading to rising internal temperatures, and under some circumstances, a second melting of the lower mantle, followed by a second freezing (e.g.,Desch and Neveu 2017). A second thaw and freeze could explain the much less eroded appearance of Vulcan Planitia and the tectonic belt separating it from Oz Terra. Hints of even more recent activity

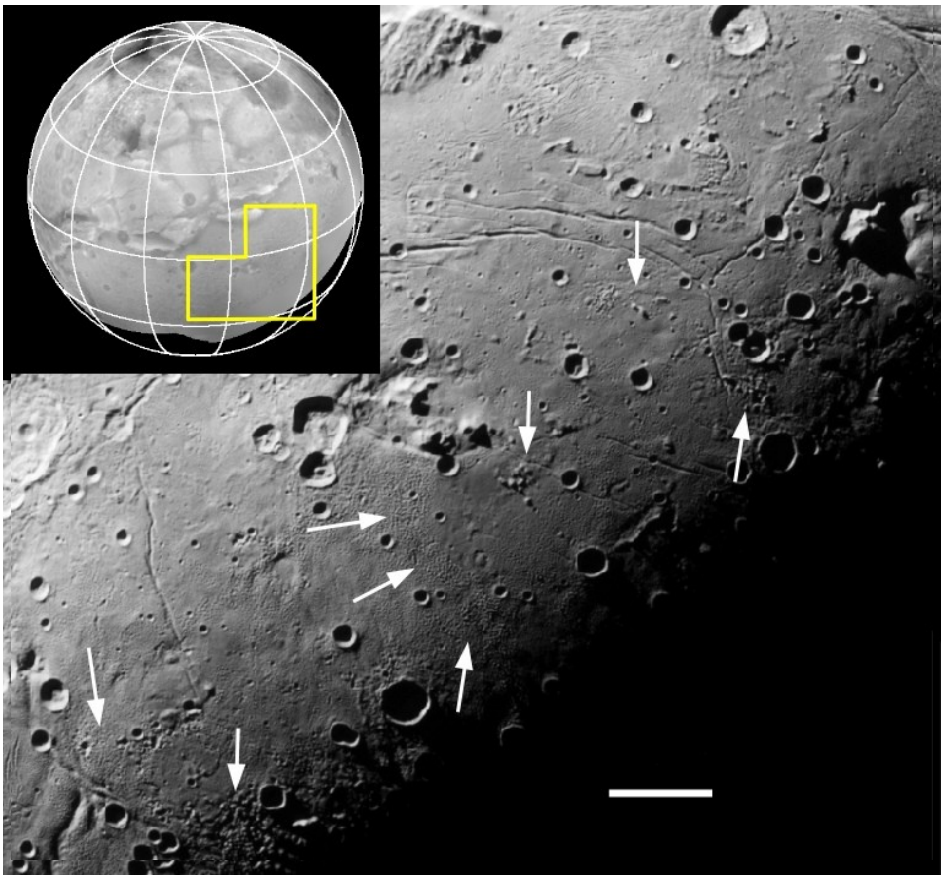

Figure 11. Clusters of small pits and hills near Charon's terminator in an MVIC panchromatic image. Kubrick Mons, one of the moated mountains, is visible at upper right. Scale bar is 50 km.

on Charon can be seen near the terminator as fields of small pits and clusters of small hills that appear to post-date the resurfacing of Vulcan Planitia (Fig. 11). These could be related to escape of volatiles, perhaps from the submerged crustal blocks. Volatiles escaping from Charon's interior could perhaps have become cold-trapped in the near surface environment before being mobilized again later when blocks of crust were overrun by warmer mantle material.

Another striking feature is Charon's dark, reddish pole, Mordor Macula (Fig. 10). This feature (along with its counterpart on the opposite pole that is barely discernible in Pluto-shine images) is hypothesized to form through a process that is still operating today, with no obvious analog elsewhere in the solar system (Grundy et al. 2016b). Gas, chiefly CH_4, escapes from Pluto and streams radially outward. Some of it passes close enough to Charon to form an extremely thin, transiently trapped atmosphere around Charon. Charon's winter pole goes without sunlight for more than a century, becoming so cold that CH_4 gas freezes out there as ice. Although the winter pole is oriented away from the Sun, is is still exposed to enough ultraviolet radiation (e.g., Gladstone et al. 2018) to convert some of the CH_4 ice into heavier hydrocarbons that remain behind after the Sun rises again, and these hydrocarbons are eventually further processed into dark, reddish, tholin-like material. Over the age of the solar system, estimates suggest some 10s of cm of this material could be produced, more than enough to paint Charon's poles, even as it is mixed down into the H_2O ice substrate via impact gardening.

Expectations for other large TNOs

Other large TNOs have abundant volatile ices. Eris and Makemake exhibit deeper CH_4 ice absorption bands than Pluto does (e.g., Licandro et al. 2006; Dumas et al. 2007; Brown et al. 2007). Subtle shifts in the wavelengths of their CH_4 bands suggest the presence of abundant N_2 too (Tegler et al. 2008, 2010). Their high albedos and abundant volatiles led Grundy and Umurhan (2017) to pose the question of whether Eris and Makemake might be "Sputnik planets" covered with thick volatile ice deposits, convectively overturning to keep their surfaces refreshed. Eris has a higher mass, density, and thus rock content than Pluto, resulting in greater internal energy from decay of long-lived radionuclides. Makemake probably has a smaller internal energy budget. Or could they be "bladed planets" with globally distributed bladed terrain? Pluto's bladed terrain has deep CH_4 ice absorptions (e.g., Earle et al. 2018) reminiscent of the spectra of Eris and Makemake.

Volatile ices have been more tentatively reported on other large TNOs, such as Sedna and Quaoar (Schaller and Brown 2007b; Barucci et al. 2010, 2015). Their much more subtle absorption features suggest far less volatile material in their surface environments, and presumably correspondingly less geological activity. Considering the gradual escape of volatiles to space (e.g., Schaller and Brown 2007a), could what is currently present be the last remnants of once abundant supplies? That idea raises questions about what sorts of features might be left behind after volatiles had played a key role in creating landforms before being lost to space. Could Triton's cantaloupe terrain be the remnant of a once vast glacier of convecting volatile ice? Triton's cantaloupe cells have similar spatial scales to the convective cells in Sputnik Planitia. What might a planetary surface look like after all the volatile ice in bladed terrain has gone away? Perhaps wind-blown debris that had accumulated between the blades would remain behind, leaving a more subdued pattern of parallel ridges. Valleys carved by volatile ice glaciers could certainly be expected to scar the landscape long after the glaciers had sublimated away and H_2O ice edifices constructed by cryovolcanic eruptions could be expected to persist, too.

Numerous even smaller dwarf planets exist in the Kuiper belt, having long since lost whatever primordial endowments of volatile ices they accreted with. But Charon teaches us that even these smaller bodies could have experienced activity in the past that may have dramatically reshaped their geology. Haumea and Orcus both show strong H_2O ice spectral features like Charon (Fornasier et al. 2004; Trujillo et al. 2007), suggestive of extensive melting and resurfacing. Smaller, darker dwarf planets might never have been resurfaced by molten H_2O, maintaining cold, primordial surfaces. But if their deep interiors ever became warm enough to collapse their initially high primordial porosities, or even melt and partially differentiate, we can expect them to have shrunk, leaving a telltale signature of compressional tectonics in their surface geology.

References

Agnor, C.B., and D.P. Hamilton 2006. Neptune's capture of its moon Triton in a binary-planet gravitational encounter. Nature 441, 192-194.

Barucci, M.A., C.M. Dalle Ore, A. Alvarez-Candal, C. de Bergh, F. Merlin, et al. 2010. (90377) Sedna: Investigation of surface compositional variation. Astron. J. 140, 2095-2100.

Barucci, M.A., C.M. Dalle Ore, D. Perna, D.P. Cruikshank, A. Doressoundiram, A. Alvarez-Candal, E. Dotto, and C. Nitschelm 2015. (50000) Quaoar: Surface compositional variability. Astron. & Astrophys. 584, A107.1-7.

Bertrand, T., F. Forget, O.M. Umurhan, W.M. Grundy, B. Schmitt, et al. 2018. The nitrogen cycles on Pluto over seasonal and astronomical timescales. Icarus 309, 277-296.

Beyer, R.A., F. Nimmo, W.B. McKinnon, J.M. Moore, R.P. Binzel, et al. 2017. Charon tectonics. Icarus 287, 161-174.

Brown, M.E., K.M. Barkume, G.A. Blake, E.L. Schaller, D.L. Rabinowitz, et al. 2007. Methane and ethane on the bright Kuiper belt object 2005 FY_9. Astron. J. 133, 284-289.

Cheng, A.F., H.A. Weaver, S.J. Conard, M.F. Morgan, O. Barnouin-Jha, et al. 2008. LOng-Range Reconnaissance Imager on New Horizons. Space Sci. Rev. 140, 189-215.

Cheng, A.F., M.E. Summers, G.R. Gladstone, D.F. Strobel, L.A. Young, et al., 2017. Haze in Pluto's atmosphere. Icarus 290, 112-133.

Cook, J.C., C.M. Dalle Ore, S. Protopapa, R.P. Binzel, D.P. Cruikshank, et al. 2019. The distribution of H_2O, CH_3OH, and hydrocarbon ices on Pluto: Analysis of New Horizons spectral images. Icarus 331, 148-169.

Croft, S.K., J.S. Kargel, R.L. Kirk, J.M. Moore, P.M. Schenk, and R.G. Strom 1995. The geology of Triton. In: D.P. Cruikshank (Eds.), *Neptune and Triton*, University of Arizona Press, Tucson, 879-947.

Cruikshank, D.P., T.L. Roush, T.C. Owen, T.R. Geballe, C. de Bergh, et al., 1993. Ices on the surface of Triton. Science 261, 742-745.

Cruikshank, D.P. 2005. Triton, Pluto, Centaurs, and transneptunian bodies. Space Sci. Rev. 116, 421-439.

Davies, J.H., and D.R. Davies 2010. Earth's surface heat flux. Solid Earth 1, 5-24.

Desch, S.J., and M. Neveu 2017. Differentiation and cryovolcanism on Charon: A view before and after New Horizons. Icarus 287, 175-186.

Dobrovolskis, A.R., and A.W. Harris 1983. The obliquity of Pluto. Icarus 55, 231-235.

Dumas, C., F. Merlin, M.A. Barucci, C. de Bergh, O. Hainault, et al. 2007. Surface composition of the largest dwarf planet 136199 Eris (2003 UB_{313}). Astron. & Astrophys. 471, 331-334.

Earle, A.M., and R.P. Binzel 2015. Pluto's insolation history: Latitudinal variations and effects on atmospheric pressure. Icarus 250, 405-412.

Earle, A.M., W. Grundy, C.J.A. Howett, C.B. Olkin, A.H. Parker, et al. 2018. Methane distribution on Pluto as mapped by the New Horizons Ralph/MVIC instrument. Icarus 314, 195-209.

Fornasier, S., E. Dotto, M.A. Barucci, and C. Barbieri 2004. Water ice on the surface of the large TNO 2004 DW. Astron. & Astrophys. 422, L43-L46.

Gladstone, G.R., W.R. Pryor, S.A. Stern, K. Ennico, C.B. Olkin, et al. 2018. The Lyman-α sky background as observed by New Horizons. Geophys. Res. Lett. 45, 8022-8028.

Grundy, W.M., R.P. Binzel, B.J. Buratti, J.C. Cook, D.P. Cruikshank, et al. 2016a. Surface compositions across Pluto and Charon. Science 351, 1283.

Grundy, W.M., D.P. Cruikshank, G.R. Gladstone, C.J.A. Howett, T.R. Lauer, et al. 2016b. Formation of Charon's red poles from seasonally cold-trapped volatiles. Nature 539, 65-68.

Grundy, W.M., and O.M. Umurhan 2017. Are Makemake and Eris sputnik planets? American Astronomical Society, DPS meeting #49, id.202.02 (abstract).

Grundy, W.M., T. Bertrand, R.P. Binzel, M.W. Buie, B.J. Buratti, et al. 2018. Pluto's haze as a surface material. Icarus 314, 232-245.

Howard, A.D., J.M. Moore, O.M. Umurhan, O.L. White, R.S. Anderson, et al., 2017a. Present and past glaciation on Pluto. Icarus 287, 287-300.

Howard, A.D., J.M. Moore, O.L. White, O.M. Umurhan, P.M. Schenk, et al. 2017b. Pluto: Pits and mantles on uplands north and east of Sputnik Planitia. Icarus 293, 218-230.

Hubbard, W.B., D.M. Hunten, S.W. Dieters, K.M. Hill, and R.D. Watson 1988. Occultation evidence for an atmosphere on Pluto. Nature 336, 452-454.

Licandro, J., W.M. Grundy, N. Pinilla-Alonso, and P. Leisy 2006. Visible spectroscopy of 2003 UB_{313}: Evidence for N_2 ice on the surface of the largest TNO? Astron. & Astrophys. 458, L5-L8.

Lunine, J.I. 1993. Triton, Pluto, and the origin of the solar system. Science 261, 697-698.

McKinnon, W.B. 1984. On the origin of Triton and Pluto. Nature 311, 355-358.

McKinnon, W.B., F. Nimmo, T. Wong, P.M. Schenk, O.L. White, et al. 2016. Convection in a volatile nitrogen-ice-rich layer drives Pluto's geological vigour. Nature 534, 82-85.

McKinnon, W.B., S.A. Stern, H.A. Weaver, F. Nimmo, C.J. Bierson, et al. 2017. Origin of the Pluto-Charon system: Constraints from the New Horizons flyby. Icarus 287, 2-11.

Moore, J.M., W.B. McKinnon, J.R. Spencer, A.D. Howard, P.M. Schenk, et al. 2016. The geology of Pluto and Charon through the eyes of New Horizons. Science 351, 1284-1293.

Moore, J.M., A.D. Howard, O.M. Umurhan, O.L. White, P.M. Schenk, et al., 2017. Sublimation as a landform-shaping process on Pluto. Icarus 287, 320-333.

Moore, J.M., A.D. Howard, O.M. Umurhan, O.L. White, P.M. Schenk, et al., 2018. Bladed terrain on Pluto: Possible origins and evolution. Icarus 300, 129-144.

Moores, J.E., C.L. Smith, A.D. Toigo, and S.D. Guzewich 2017. Penitentes as the origin of the bladed terrain of Tartarus Dorsa on Pluto. Nature 541, 188-190.

Neufeld, M.J. 2014. First mission to Pluto: Policy, politics, science, and technology in the origins of New Horizons, 1989-2003. Historical Studies in the Natural Sciences 44, 234-276.

Neveu, M., S.J. Desch, and C.R. Glein 2015. Prerequisites for explosive cryovolcanism on dwarf planet-class Kuiper belt objects. Icarus 246, 48-64.

Nimmo, F., O. Umurhan, C.M. Lisse, C.J. Bierson, T.R. Lauer, et al., 2017. Mean radius and shape of Pluto and Charon from New Horizons images. Icarus 287, 12-29.

Nogueira, E., R. Brasser, and R. Gomes 2011. Reassessing the origin of Triton. Icarus 214, 113-130.

Olkin, C.B., J.R. Spencer, W.M. Grundy, A.H. Parker, R.A. Beyer, et al. 2017. The global color of Pluto from New Horizons. Astron. J. 154, 258.1-13.

Owen, T.C., T.L. Roush, D.P. Cruikshank, J.L. Elliot, L.A. Young, et al. 1993. Surface ices and atmospheric composition of Pluto. Science 261, 745-748.

Protopapa, S., W.M. Grundy, D.C. Reuter, D.C. Hamilton, C.M. Dalle Ore, et al. 2017. Pluto's global surface composition through pixel-by-pixel Hapke modeling of New Horizons Ralph/ LEISA data. Icarus 287, 218-228.

Reuter, D.C., S.A. Stern, J. Scherrer, D.E. Jennings, J.W. Baer, et al. 2008. Ralph: A visible/infrared imager for the New Horizons Pluto/Kuiper belt mission. Space Sci. Rev. 140, 129-154.

Schaller, E.L., and M.E. Brown 2007a. Volatile loss and retention on Kuiper belt objects. Astrophys. J. 659, L61-L64.

Schaller, E.L., and M.E. Brown 2007b. Detection of methane on Kuiper belt object (50000) Quaoar. Astrophys. J. 670, L49-L51.

Schenk, P.M., and K. Zahnle 2007. On the negligible surface age of Triton. Icarus 192, 135-149.

Schenk, P.M., R.A. Beyer, W.B. McKinnon, J.M. Moore, J.R. Spencer, et al., 2018a. Basins, fractures, and volcanoes: Global cartography and topography of Pluto from New Horizons. Icarus 314, 400-433.

Schenk, P.M., R.A. Beyer, W.B. McKinnon, J.M. Moore, J.R. Spencer, et al. 2018b. Breaking up is hard to do: Global cartography and topography of Pluto's mid-sized icy moon Charon from New Horizons. Icarus 315, 124-145.

Schmitt, B., S. Philippe, W.M. Grundy, D.C. Reuter, R. Côte, et al. 2017. Physical state and distribution of materials at the surface of Pluto from New Horizons LEISA imaging spectrometer. Icarus 287, 229-260.

Smith, B.A., L.A. Soderblom, D. Banfield, C. Barnet, A.T. Basilevksy, et al., 1989. Voyager 2 at Neptune: Imaging science results. Science 246, 1422-1449.

Stern, S.A., F. Bagenal, K. Ennico, G.R. Gladstone, W.M. Grundy, et al., 2015. The Pluto system: Initial results from its exploration by New Horizons. Science 350, 292.

Stern, S.A., R.P. Binzel, A.M. Earle, K.N. Singer, L.A. Young, et al. 2017. Past epochs of significantly higher pressure atmospheres on Pluto. Icarus 287, 47-53.

Tegler, S.C., W.M. Grundy, F. Vilas, W. Romanishin, D.M. Cornelison, et al. 2008. Evidence of N_2-ice on the surface of the icy dwarf Planet 136472 (2005 FY_9). Icarus 195, 844-850.

Tegler, S.C., D.M. Cornelison, W.M. Grundy, W. Romanishin, M.R. Abernathy, et al. 2010. Methane and nitrogen abundances on Pluto and Eris. Astrophys. J. 725, 1296-1305.

Trafton, L.M., D.L. Matson, and J.A. Stansberry 1998. Surface/atmosphere interactions and volatile transport (Triton, Pluto, and Io). In: B. Schmitt, C. de Bergh, M. Festou (Eds.), *Solar System Ices*, Kluwer Academic, Dordrecht, 773-812.

Trowbridge, A.J., H.J. Melosh, J.K. Steckloff, and A.M. Freed 2016. Vigorous convection as the explanation for Pluto's polygonal terrain. Nature 534, 79-81.

Trujillo, C.A., M.E. Brown, K.M. Barkume, E.L. Schaller, and D.L. Rabinowitz 2007. The surface of 2003 EL_{61} in the near-infrared. Astrophys. J. 655, 1172-1178.

Tyler, G.L., D.N. Sweetnam, J.D. Anderson, S.D. Borutzki, J.K. Campbell, et al., 1989. Voyager radio science observations of Neptune and Triton. Science 246, 1466-1473.

Umurhan, O.M., A.D. Howard, J.M. Moore, A.M. Earle, O.L. White, et al., 2017. Modeling glacial flow on and onto Pluto's Sputnik Planitia. Icarus 287, 301-319.

White, O.L., J.M. Moore, W.B. McKinnon, J.R. Spencer, A.D. Howard, et al. 2017. Geological mapping of Sputnik Planitia on Pluto. Icarus 287, 261-286.

Acknowledgment

This work was supported by NASA's New Horizons project.